

EFFECTS OF CONSOLIDATION TEMPERATURE, STRENGTH AND MICROSTRUCTURE ON FRACTURE TOUGHNESS OF NANOSTRUCTURED FERRITIC ALLOYS—P. Miao, G. R. Odette, T. Yamamoto (University of California, Santa Barbara), M. Alinger (University of California, Santa Barbara, University of California, Berkeley), D. Hoelzer (Oak Ridge National Laboratory), and D. Gragg (University of California, Santa Barbara)

OBJECTIVE

This work is to investigate fracture toughness of hot-isostatic-processed (HIPed) nanostructured ferrite alloys and the effects of HIPing parameters and microstructures on the fracture toughness.

SUMMARY

Fully consolidated nanostructured ferritic alloys (NFAs) were prepared by attritor milling pre-alloyed Fe-14Cr-3W-0.4Ti and 0.3wt% Y_2O_3 powders, followed by hot isostatic pressing (HIPing) at 1000°C and 1150°C and 200 MPa for 4 h. Transmission electron microscopy (TEM) revealed similar bimodal distributions of fine and coarse ferrite grains in both cases. However, as expected, the alloy microhardness decreased with increasing in HIPing temperature. Three point bend tests on single edge notched specimens, with a nominal root radius $\rho = 0.15$ mm, were used to measure the notch fracture toughness, K_{Ic} , as a function of test temperature. The K_{Ic} curves were found to be similar for both alloys. It appears that the coarser ferrite grains control cleavage fracture, in a way that is independent of alloy strength and HIPing temperature.

PROGRESS AND STATUS

Introduction

Nanostructured ferritic alloys (NFAs) containing 12 to 14%Cr and a very high density of nm-scale Y-Ti-O precipitate phases have outstanding low temperature tensile (> 1 GPa) and high temperature creep strengths [1-3] and offer a potential for mitigating radiation damage, including the effects of high helium levels [4, 5] in fusion reactor structures. However, a significant challenge to the development of NFAs is maintaining adequate fracture toughness, in combination with high strength. Various approaches to optimizing the fracture toughness of NFAs, including alternative processing paths [5-7] and alloy designs [5, 8], have been, or are being, studied.

Previous investigations [1] of the fracture toughness of an extruded MA957 NFA revealed a strong dependence on microstructural anisotropy. This anisotropy is manifested as elongated grains in the extrusion direction, with a length to diameter aspect ratio of ≈ 10 -20 [7], along with preferred longitudinal $\langle 110 \rangle$ -fiber texture [9]. This MA957 heat alloy also contained Al_2O_3 impurity inclusion stringers that were elongated in the extrusion direction. As a result, orientations with the crack plane normal perpendicular to the extrusion direction (C-R and C-L) have lower toughness. The lowest toughness is when the cracks grow in the extrusion direction (C-L). In contrast, the toughness is higher and transition temperature (TT) is lower when the crack plane normal is parallel to the extrusion direction (L-R). Thus, the purpose of this study was to evaluate the toughness in a nominally clean (inclusion free), isotropic and equiaxed alloys produced by HIPing.

Experimental Procedure

The NFAs were prepared by mechanically alloying Fe-14Cr-3W-0.4Ti powder with 0.3wt% Y_2O_3 for 40h in an attritor mill with an argon atmosphere. The milled powders were then vacuum canned and consolidated by HIPing at 200MPa for 4h at 1000°C (14YWT1000) and 1150°C (14YWT1150). The alloy densities were measured using a MicroMeritics AccuPyc 1330 pycnometer. Their potential porosity was examined by optical microscopy. The microstructure of the alloy was characterized by TEM (JEOL2010HR). The TEM specimens were prepared by grinding 3mm diameter discs to a thickness of

~0.15mm, followed by thinning to electron transparency in a TENUPOL twin-jet electro-polisher with $H_2SO_4 + 80\%CH_3OH$ at room temperature.

The flow strength of the NFAs was evaluated by diamond pyramid Vicker's microhardness (DPH) measurements using a 1kg load at room (~23°C) and liquid-nitrogen (-196°C) temperatures. Notch fracture toughness was measured in three-point-bending on an MTS servohydraulic load frame at a displacement rate of 0.08mm/min over the temperature range from -100°C to 205°C. The fracture specimens (B=1.65, W=3.3 and L = 18 mm) were by EDM notched with a 0° flank angle to an $a/W \approx 0.5$ with a nominal root radius $r = 0.15$ mm that was then razor-press sharpened prior to testing. However, since they were not fatigue pre-cracked, the sharp *notch* fracture toughness is designated as K_{Ic} . Fractographic characterization was carried out using a SEM FEI XL-40.

Results and Discussion

The densities of 14YWT1000 and 14YWT1150 were 7.91 ± 0.02 and 7.92 ± 0.06 , respectively, indicating full consolidation. For example, the density of a wrought alloy with a similar composition (~81wt%Fe, 13%Cr, 3%W) is 7.86 g/cm^3 [10]. This conclusion was further supported by the failure to observe porosity by optical microscopy.

TEM showed similar, roughly 50-50% fine and coarse ferrite mixture of ferrite grains (see Figures. 1a and c) in both 14YWT1000 and 14YWT1150. The fine ferrite grains are ~200 nm in diameter. The coarser grains have wide size distribution, ranging from about one to several tens of μm . The larger ferrite grains are presumably the result of recovery and growth in regions with a lower density of fine scale precipitates phases, including both nm scale Y-Ti-O clusters and slightly larger $Ti_2Y_2O_7$ pyrochlore oxides [11]. Similar bimodal distributions have also been observed in ODS Eurofer [12]. Dislocation densities in the fine ferrite grains are higher than in the coarse grains (Figures 1b and d).

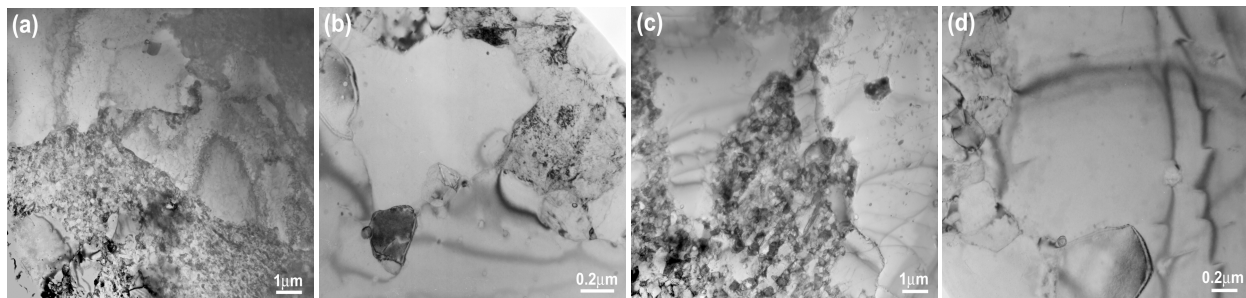


Figure 1. Microstructure of (a) and (b) 14YWT1000 and (c) and (d) 14YWT1150 at low (a and c) and medium (b and d) resolution.

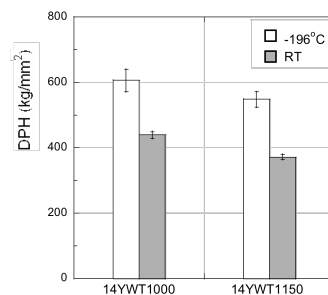


Figure 2. The effect of the HIPing temperature on microhardness.

As shown in Figure 2, hardness at room temperature and -196°C decreases with increasing in HIPing temperature. These results are reasonably consistent with previous data on similar alloys reported by Alinger et al [5, 13], who found that the nano-sized particles sizes increase and their number densities decrease with higher HIPing temperature. The similarity in the grain structures in 14YWT1000 and 14YWT1150 suggests that the recovery and grain growth is resisted in regions with high nano-scale particle densities in both cases.

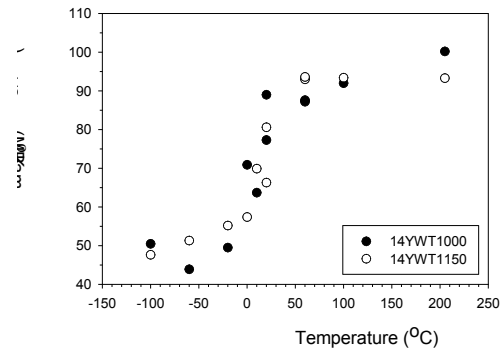


Figure 3. The variation of K_p with temperature for 14YWT1000 and 14YWT1150.

The variation of the K_p of 14YWT1000 and 14YWT1150 with temperature is shown in Figure 3. Although the strengths of these alloys are different, their TT of $\approx 10^{\circ}\text{C}$ and $K_p(T)$ curves are nearly identical.

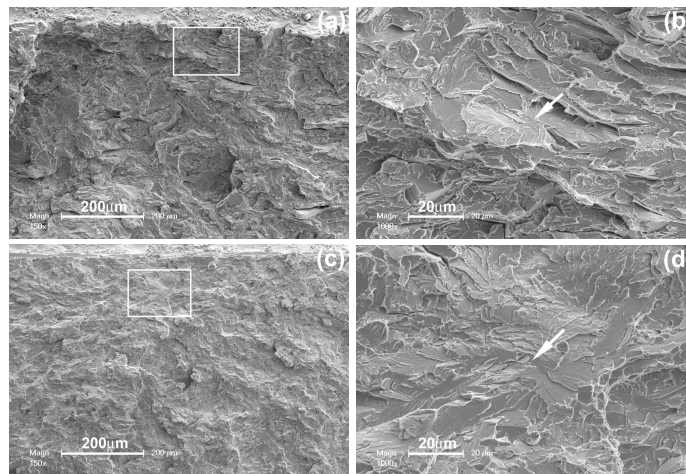


Figure 4. Low (a and c) and intermediate (b and d) magnification fractographic images of 14YWT1000 (a and b) 14YWT1150 (c and d) specimens fractured at -100°C .

These results may suggest that the bimodal grain structure may be more important than strength in controlling fracture in these NFAs. Fractographic observations support this hypothesis. Figures 4 and 5 show fracture on the lower shelf at -100°C by pure cleavage (Figure 4), and by a ductile microvoid nucleation, growth and coalescence on the upper-shelf at 200°C (Figure 5). However, even at the higher temperatures, isolated cleavage facets are observed. Higher magnification examination of suspected initiation sites (framed and arrowed in Figures 4) at -100°C suggest that the cleavage is triggered by the fracture of large particles or, perhaps extra hard grains, surrounded by facet sizes that are larger than ≈ 5 to $10\ \mu\text{m}$, consistent with the corresponding sizes of the coarser ferrite grains. The conclusion is even

clearer in the fractographs shown in Figure 5 showing disproportionate importance of the larger grains in cleavage fracture at 200°C.

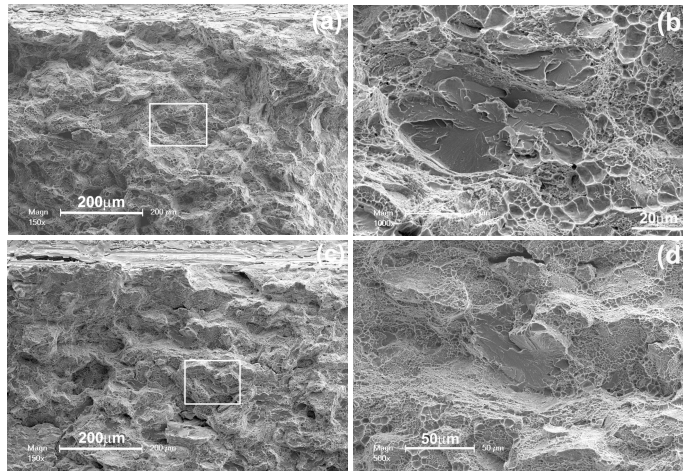


Figure 5. Low (a and c) and intermediate (b and d) magnification fractographic images of 14YWT1000 (a and b) 14YWT1150 (c and d) specimens fractured at 200°C.

Discussion

The breakdown in the usual higher strength-lower toughness relation is not fully understood. One possibility is that dislocation pile-ups in the larger and softer coarse grains trigger cleavage, perhaps by fracturing smaller harder grains or brittle particles. In this case, differences in the average strength of the alloy may be less significant than similarities in the grain structures. Indeed, if the larger grains are softer, the effect on the size of the pile up may offset the corresponding effect of higher strength.

Nano-indentation studies will be used to explore strength variations between larger and smaller grains. Additional studies to characterize the NFAs nano-microstructures, constitutive properties and sharp fatigue pre-crack fracture toughness are ongoing. Note this study will be extended to HIPing at 850°C, which was part of the original test matrix; however, due to a failure in the HIP in this case, the resulting 14YWT850 alloy, with a DPH of $588 \pm 25 \text{ kg/mm}^2$, was not fully consolidated. Hence, the 14YWT850 was not fracture tested.

These preliminary results suggest that producing alloys with a more uniform and finer distribution of grain sizes would lead to higher toughness and lower TT. Of course, developing processing routes that lead to more homogeneous nano-microstructures is a more generally desirable objective.

Concluding Remarks

High density, pore-free 14YWT NFAs were processed by HIPing mechanically alloyed powders at 1000°C and 1150°C. Both alloys contained similar distributions of fine ($\approx 200\text{nm}$) and coarse (one to several tens of μm) ferrite grains. The 14YWT1000 is substantially stronger than 14YWT1150, as expected. However, both alloys have similar notch fracture toughness with a TT $\approx 10^\circ\text{C}$. We hypothesize that the toughness is primarily mediated by the coarser ferrite grains in a way that is relatively insensitive to the alloy strength. Processing paths that produce finer and more homogeneous microstructures offer the promise of higher toughness, along with an optimized balance of properties.

References

- [1] M. J. Alinger, G. R. Odette, and G. E. Lucas, *J. Nucl. Mater.* 307-311 (2002) 484.
- [2] R. L. Klueh, J. P. Shingledecker, R. W. Swindeman, and D. T. Hoelzer, *J. Nucl. Mater.* 341 (2005) 103.
- [3] R. L. Klueh, P. J. Maziasz, I. S. Kim, L. Heatherly, D. T. Hoelzer, N. Hashimoto, E. A. Kenik, and K. Miyahara, *J. Nucl. Mater.* 307-311 (2002) 773.
- [4] T. Yamamoto et al., *Journal of Nuclear Materials* (to be published).
- [5] M. J. Alinger, G. R. Odette, and D. T. Hoelzer, *J. Nucl. Mater.* 329-333 (2004) 382.
- [6] S. Ukai and M. Fujiwara, *J. Nucl. Mater.* 307-311 (2002) 749.
- [7] A. Alamo, V. Lambard, X. Averty, and M. H. Mathon, *J. Nucl. Mater.* 329-333 (2004) 333.
- [8] T. Kuwabara, H. Kurishita, S. Ukai, M. Narui, and S. Mizuta, *J. Nucl. Mater.* 258-263 (1998) 1236.
- [9] T. S. Chou and H.K.D.H. Bhadeshia, *Metall. Trans.* 24A (1993) 773.
- [10] C. T. Lynch, *CRC Handbook of Materials Science*, CRC Press, Cleveland, Ohio, 1974, Vol. 2, 105.
- [11] H. Kishimoto, M. J. Alinger, G. R. Odette, and T. Yamamoto, *J. Nucl. Mater.* 329-333 (2004) 369.
- [12] C. Cayron, E. Rath, I. Chu, and S. Launois, *J. Nucl. Mater.* 335 (2004) 83.
- [13] M. J. Alinger, Ph.D. dissertation, University of California, Santa Barbara, 2004.